Cooperative Multichannel Directional Medium Access Control for Ad Hoc Networks

Yu Wang, Mehul Motani, *Senior Member, IEEE*, Hari Krishna Garg, Qian Chen, *Member, IEEE*, and Tie Luo, *Member, IEEE*

***Abstract*—A cooperative multichannel directional medium access control (CMDMAC) protocol incorporating minor-lobe interference is proposed for directional ad hoc networks. While most existing MAC protocols require either extra equipment or clock synchronization to address deafness and directional hidden terminal problems, CMDMAC requires neither to solve these problems. Observing that directional transmission assumes single data channel in most instances, CMDMAC incorporates directional and multichannel transmissions to deliver superior networking performance. Theoretical analysis for CMDMAC is provided, and its performance is validated via NS-2 simulation. We compare CMDMAC with a noncooperative version, which is called NCDMAC, and observe a throughput improvement of around 15% and 56% in the single-data-channel and multiple-data-channel scenarios, respectively. We examine CMDMAC under mobile scenarios and observe throughput degradations of around 11% and 15% compared with the static single-data-channel and multiple-data-channel scenarios, respectively. We also compare CMDMAC with other popular directional and multichannel MAC protocols, and the results show that CMDMAC outperforms all of them.**

***Index Terms*—Ad hoc networks, cooperation, directional antennas, medium access control (MAC), multichannel.**

I. Introduction

SINCE directional transmission can provide higher data rates, omni-directional networks are falling into disfavor especially in new networking applications, such as high definition video streaming. In this paper, we work on directional MAC protocols for ad hoc networks. Two key challenges in designing directional MAC protocols for ad hoc networks are the hidden terminal and deafness problems. Existing solutions are generally based on one of two approaches, namely i) networkwide synchronization and ii) multiple radios with one radio dedicated for control messages. However, synchronization is difficult to achieve in ad hoc networks. Besides, we can not expect all terminals to be equipped with two or more radios in the emerging IoT, M2M or other heterogeneous networks, as smart phones with multiple Wireless Fidelity (WiFi) radios are seldom seen in the market. Another scenario where multiple radios may not be available for each terminal is sensor network, since there will be strict concern about hardware size and power consumption.

The main focus of this paper is on designing a directional MAC that can solve hidden terminal and deafness problems without network-wide synchronization and multiple radios for directional ad hoc networks. With the objective of improving aggregate throughput for directional ad hoc networks, we propose a cooperative multichannel directional medium access control (CMDMAC) protocol. Multichannel and directional transmissions are two known multiplexing techniques that can be used to improve networking performance. However, they are studied separately in most literature on MAC protocols due to complexity considerations. CMDMAC incorporates multi-data-channel transmission to further improve networking performance. Each terminal is assumed to be equipped with a single half-duplex radio, which may be tuned to different channels. To solve hidden terminal and deafness problems under a multichannel directional environment, CMDMAC operates with one control channel and multiple data channels and uses cooperation among neighbors. All control messages are exchanged omnidirectionally in control channel, whereas data packets are transmitted directionally in data channels. Moreover, a single radio is not a necessary condition for CMDMAC. Terminals equipped with multiple radios may also perform CMDMAC.

The main contributions of this work are as follows.

1) A new MAC protocol, which is termed CMDMAC, is proposed for multichannel directional ad hoc networks, which requires neither additional hardware nor synchronization.
2) Deafness and hidden terminal problems for multichannel directional ad hoc networks are solved with cooperative methods.
3) Theoretical analysis and extensive NS-2 simulation results for evaluating CMDMAC are presented.

The rest of this paper is organized as follows. In Section II, related work is reviewed. In Section III, the system model is introduced. In Section IV, we discuss the problems and challenges in directional and multichannel MAC design. In Section V, we present the details of the proposed CMDMAC protocol. In Section VI, we present a theoretical analysis for CMDMAC. In Section VII, we evaluate the performance of CMDMAC and compare with other MAC protocols via simulations. Conclusions are drawn in Section VIII.

Manuscript received January 12, 2015; revised June 16, 2015; accepted September 4, 2015. This work was supported by the Singapore National Research Foundation under its International Research Centre at Singapore Funding Initiative and administered by the Interactive Digital Media Programme Office.

Y. Wang, M. Motani, and H. K. Garg are with the Department of Electrical and Computer Engineering, National University of Singapore, Singapore 119077 (e-mail: wangyu86@u.nus.edu; elemm@nus.edu.sg; eleghk@nus.edu.sg).

Q. Chen and T. Luo are with the Institute for Infocomm Research, Singapore 138632 (e-mail: qchen@i2r.a-star.edu.sg; luot@i2r.a-star.edu.sg).

Digital Object Identifier 10.1109/JSYST.2015.2478801

This article has been accepted for inclusion in a future issue of this journal. Content is final as presented, with the exception of pagination.

II. Literature Review

In the area of directional MAC protocols, Takai *et al.*, in their pioneering work [2], first proposed methods such as directional virtual carrier sensing. In [3], the authors summarized the key design problems in directional MAC; however, not all issues were solved satisfactorily. In [4], it was argued that directional MAC with practical antenna models needed more attention. In [5], it was found that existing solutions rarely deal with the impact of minor lobes and they proposed a MAC protocol based on network-wide synchronization. In [6], a radio dedicated for control messages was used to solve the hidden terminal problem. In [7], the authors proposed a protocol using sector sweep to collect neighbor information for directional networks. In [8], double radios were used to identify deaf terminals. In [9], data frames were fragmented to reduce packet collisions but only hidden terminals in the main sectors of the communicating pairs were eliminated. In [10], a protocol was proposed where an additional busy tone equipment was needed for each terminal. In [12], a contention window was used for terminals to negotiate and solve the hidden terminal problem. There also exist several research papers on providing efficient directional MACs for 60 GHz personal networks [11].

In existing studies on multichannel MAC, there are two main approaches to solving hidden terminal and deafness problems. The first one is to use multiple radios and dedicate one of them for control channel messages [13], [14]. It is clear that the hardware complexity is increased in this approach, and hence cost and energy consumption as well. We also cannot expect that all terminals will be equipped with multiple radios in a heterogeneous network. In fact, we seldom find a smartphone with two WiFi radios. The other approach consists in regulating the irregular nodes' behavior by using contention time slots [15], [16] or channel hopping sequences [17]. However, this approach requires network-wide synchronization, which is a difficult task for multihop ad hoc networks [18].

In most cases, cooperation in wireless networks refers to relay data frame for neighboring terminals. The cooperative MAC for coordinating this kind of data relaying has been studied in [19]–[21]. However, most of the researchers ignore the fact that the neighboring terminals can do more than data relaying. In [22], cooperative asynchronous multichannel MAC (CAMMAC) was proposed, and cooperation was used to solve the multichannel collision problem in omnidirectional networks. In CAMMAC, nodes use two-hop topology information to tell whether two omnidirectional links can coexist in certain channel. Since directional transmission is taken into consideration in CMDMAC, the condition for two links to coexist becomes different. The contribution of CMDMAC is to extend CAMMAC to solve hidden terminal problem in directional networks. Nodes with CMDMAC have to jointly consider channel usage information, direction information, and topology information to decide whether a new link under negotiation procedure can be established or not. Methods are also known for providing efficient multichannel MACs for cognitive ratio networks [23]–[26].

In this paper, we propose CMDMAC that combines directional and multi-channel transmission. It does not require any additional hardware for control message exchange. Further, it may work asynchronously. While part of this work has been published in [1], the theoretical analysis is newly added in this paper. Moreover, the protocol is tested from more aspects via simulation.

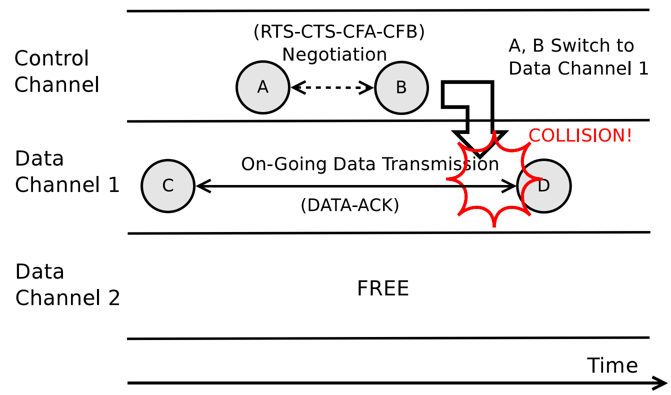

Fig. 1. System model illustration and the multichannel hidden terminal problem.

III. System Model

Here, we introduce the network and antenna model employed in this paper.

An asynchronous ad hoc network, which works in the unlicensed band, for example, the industrial, scientific and medical (ISM) band, is considered. Terminals are randomly located, and each of them is equipped with a single half-duplex transceiver. Terminals and nodes are used interchangeably henceforth. As shown in Fig. 1, multiple independent channels are available: one is dedicated for the exchange of omnidirectional control messages; others are used for the transmission of directional data packets. We further assume that radios can work in both omnidirectional and directional modes [4], [5] and that radios can be tuned among different channels [23], [24].

A two-ray propagation model is used. The received power P_R is given by

$$P_R = \frac{P_T \cdot G_T \cdot G_R \cdot H_T^2 \cdot H_R^2}{D^4} \tag{1}$$

where P_T is the transmission power, G_T is the antenna gain of transmitter (Tx), G_R is the antenna gain of receiver (Rx), H_T is the height of the Tx's antenna, H_R is the height of the Rx's antenna, and D is the distance between the Tx and the Rx.

We employ the most widely used directional antenna model [27], as shown in Fig. 2(a). The antenna gain for minor lobe is a nonzero value, i.e., 0.4, in this example, whereas the antenna gain for main lobe is much larger than 1. Both minor and main lobes have uniform antenna gains. The antenna consists of M nonoverlapping sectors. For example, M is equal to 6 in Fig. 2(b). Moreover, the antenna is capable of switching among different sectors without any switching delay [7], [12]. Direction of arrival (DoA) technique is assumed to be used, and terminals can estimate the direction of the received signal [5].

IV. Problems in Multichannel Directional MAC

The first problem is multi-channel directional hidden terminal problem. The directional hidden terminal problem with a

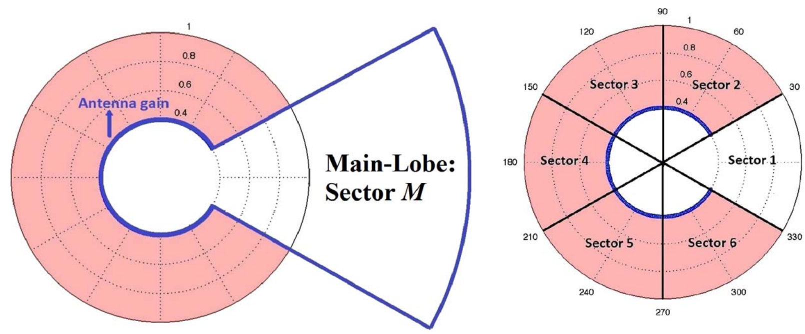

(a) (b)

Fig. 2. Antenna model. (a) Antenna gains model. (b) Antenna sector model.

single data channel is illustrated as follows. In Fig. 3, nodes A, B, C and D are engaged in data transmission while nodes E and F establish their link. After transmissions in links 1 and 2, B wants to transmit to C. Without knowing the existence of link 3, the new directional link may cause collision to E. This kind of problem is defined as directional hidden terminal problem. The multi-channel hidden terminal problem with omni-directional transmission is discussed as follows. In Fig. 1, nodes A and B are carrying out the negotiation in the control channel without knowing that C and D are communicating in data channel 1. Meanwhile, data channel 2 is free. If A and B switch to data channel 1 for data transmission, it is obvious that they may bring collision to the current link of C and D. Therefore, it is important to coordinate different terminals in the network. This kind of hidden terminal problem is defined as multi-channel hidden terminal problem. The situation studied in this paper is a combination of above two cases. We term it "multi-channel directional hidden terminal problem". Direction and channel together determine whether a node may become hidden terminal towards another terminal. For the case shown in Fig. 3, let's assume there are two data channels. The red curve indicates the transmission range of node B. If the new link 4 is in data channel 2 while link 3 is in data channel 1, there will be no collision. For the case in Fig. 1, let's assume A, B, C and D are located as two parallel link, like links 4 and 5 in Fig. 3. Even if the link of C and D is in data channel 1, there will be no collision since A and B are not in the interference range of C and D hence the two links can co-exist.

The second problem is vulnerability of receivers. Vulnerability of receivers means interference from all directions can interrupt the on-going data reception. Readers who are interested in this please refer to [1]. For the deafness problem and collision due to different gains, readers can refer to [7] for details.

V. CMDMAC Protocol Design

Here, CMDMAC will be presented in detail. The basic idea of CMDMAC is information sharing. A dedicated control channel is used while multiple data channels may exist. A four-step negotiation procedure is designed to work on the control channel, as shown in Fig. 4. The detail illustration in Fig. 4 is provided in Section V-C. With successful negotiation, terminals switch to the selected data channel for data transmission. The terminals will switch back to control channel after the data transmission is completed. The unique feature of CMDMAC is that terminals use their local channel usage records to help Txs and Rxs make decisions and prevent packet conflicts. Moreover, power adaption is used to ensure the transmission ranges in control and data channels to be the same to reduce the collision due to different gains.

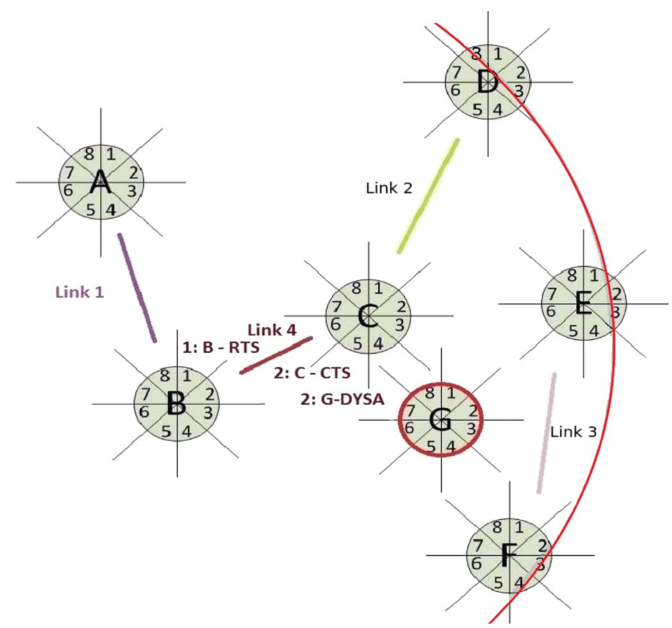

Fig. 3. Illustration of directional hidden terminal problem and cooperation.

In the remaining part of this section, related designs for CMDMAC are described along with detailed negotiation procedure.

A. Frame Structure

The formats of all frames are shown in Fig. 5. Request to send (RTS) and clear to send (CTS) are used to initialize negotiation. In RTS/CTS, the expected data channel and sector are included in channel number (CH_NO) and sector number (SEC_NO), respectively. The neighbors who hear the RTS/CTS may know which data channel and sector the negotiating pairs expect to use. Moreover, they also update neighbor information tables (NITs) based on the received information. Confirm Type A (CFA) and confirm Type B (CFB) are used to confirm reception of CTS and CFA. In CFA/CFB, the duration of link

This article has been accepted for inclusion in a future issue of this journal. Content is final as presented, with the exception of pagination.

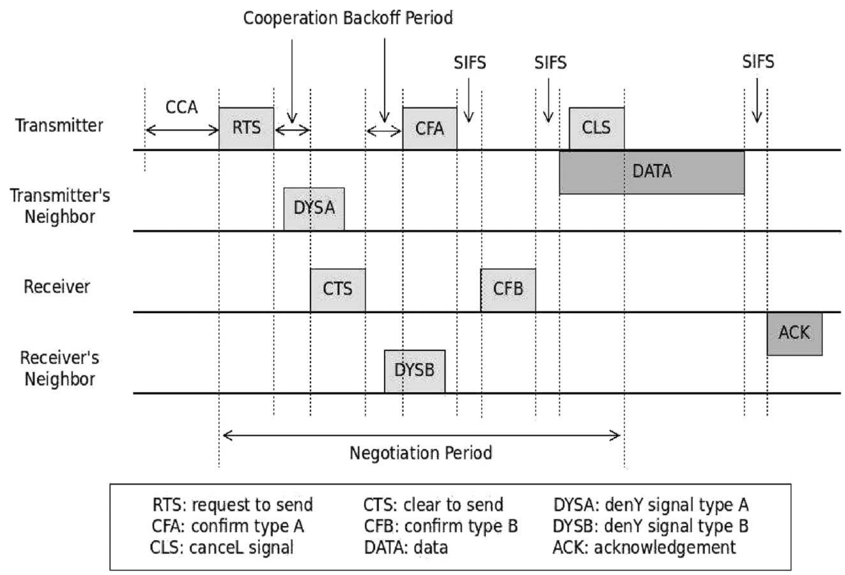

Fig. 4. Negotiation procedures and data channel handshake of CMDMAC.

RTS/CTS

FC (2 bytes)	TX_ADDR (6 bytes)	RX_ADDR (6 bytes)	CH_NO (1 bytes)	SEC_NO (1 bytes)	SEQ_NO (1 bytes)	FCS (2 bytes)

DYSA/DYSB

FC (2 bytes)	TX_ADDR (6 bytes)	RS_ADDR (6 bytes)	RS_CHSEC (2 bytes)	LTIME (2 bytes)	UP_ADDR (6 bytes)	UP_SEC (1 bytes)	FCS (2 bytes)

CFA/CFB

FC (2 bytes)	UP_ADDR (6 bytes)	UP_SEC (1 bytes)	TIME (2 bytes)	SEQ_NO (1 bytes)	FCS (2 bytes)

ACK/CLS

FC (2 bytes)	SEQ_NO (1 bytes)	FCS (2 bytes)

Abbreviation List:

FC: frame control	TX_ADDR: transmitter address	RX_ADDR: receiver address
CH_NO: channel number	SEC_NO: sector number	SEQ_NO: sequence number
FCS: frame check sequence	RS_ADDR: reason node address	RS_CHSEC: active sector and channel
LTIME: left time	UP_ADDR: updated node address	UP_SEC: updated node sector

Fig. 5. Frame structures of CMDMAC.

is included in TIME. The neighbors who hear these frames can update their directional network allocation vector (DNAV) according to their local clocks. Furthermore, updated node address (UP_ADDR) and updated node sector (UP_SEC) are used to update the NITs. Deny signal Type A (DYSA) and deny signal Type B (DYSB) are used by cooperators to stop current negotiation. Neighbors who know the channel usage information around current Tx or Rx and help in its negotiation procedure are called cooperators. In DYSA/DYSB, reason node address (RS_ADDR) identifies the active node who leads to this "veto" frame, and left time (LTIME) shows the remaining active time of the corresponding link. Acknowledgment (ACK) is the same as in IEEE 802.11 protocol. In some special cases, Tx sends CFA but receives no CFB, which means that this is an unsuccessful negotiation. Then, cancel signal (CLS) is sent by Tx to announce the cancellation of confirmation, e.g., CFA, to Tx's neighbors. CLS has the same structure as ACK.

Node Index	1-Hop Information: Neighbor Index (Sector, Up-Close)
G	E(2, 0), F(4, 0), B(7, 0), C(8, 1)
E	F(5, 0), G(6, 0), C(6, 0), D(8, 0)
F	E(1, 0), G(8, 0), C(8, 0)
B	C(2, 0), E(2, 0), G(3, 0), A(8, 0)
C	D(1, 0), E(2, 0), G(4, 1), F(4, 0), B(6, 0), A(7, 0)

Fig. 6. NIT.

B. NIT

An NIT, which contains two-hop neighbors' relative location information, is maintained by each terminal. An example is shown in Fig. 6 according to node G in Fig. 3. A to G are all wireless nodes. Take C(8, 1) in node index G's row as an instance: 8 means that C is in G's Sector 8, and 1 means that C is G's up-close neighbor. We say that two neighboring nodes are up close if they can interfere with each other through their minor lobes (and set up-close = 1). Now, let us assume that C is transmitting in the data channel with Sector 6 and G is receiving in the data channel with Sector 4 in Fig. 3. That is, they do not use their main lobes to point toward each other. As they are up-close nodes, the minor lobe of C can still interfere with G's current reception. A node can build its one-hop NIT by receiving frames from neighboring nodes with DoA and broadcast this information within the management frames. Thus, all the nodes can build the two-hop NIT.

For the static topology in this paper, we assume that two-hop neighbor information is provided by the management frames of an upper layer protocol. For the mobile topology, we assume that initial two-hop neighbor information is only provided once by the management frames at the beginning of network establishment. After the initial set up, nodes update the sector information for their neighbors using control frames. In RTS/CTS, transmitter TX_ADDR indicates the relative direction SEC_NO for neighbor RX_ADDR. Thus, terminals that receive RTS/CTS can update the corresponding neighbor information for this transmitter TX_ADDR. Similarly, if DYSA/DYSB is received, neighbor information for TX_ADDR can be updated based on UP_ADDR and UP_SEC. That is, terminal UP_ADDR is in sector UP_SEC of transmitter TX_ADDR. Same information update procedure is also implemented in CFA/CFB. Each node keeps a local table to record nonupdated duration for all its neighbors. We use two factors to decide which neighbor to be updated in the current frame: 1) whether the neighbor's direction information changed recently and 2) the time that has lapsed since last update. If there is no neighbor that satisfies factor 1, then 2 can finalize the decision. If there is one neighbor that satisfies factor 1, then this neighbor is updated. If there are multiple neighbors that satisfy factor 1, the one that has waited for the longest time is updated.

C. Negotiation Procedure for Link Establishment

Cooperation is used in CMDMAC to solve the directional multichannel hidden terminal problem. The basic idea of cooperation is information sharing among Tx, Rx, and cooperators. If a cooperator knows that Tx or Rx is negotiating for an occupied channel resource, it may deny this negotiation and provide suggestion on channel selection.

A four-way handshake procedure is performed in the control channel, as shown in Fig. 4. A Tx with CMDMAC verifies the absence of other traffic before transmitting based on carrier sense multiple access (CSMA). The Tx then initializes a negotiation by sending an RTS. DNAV is a record about channel occupation. It provides information on whether there is any transmitting or receiving node in the direction under certain channel during specific period. Readers can refer to [2] for details of DNAV. Upon receiving the RTS, the Rx checks its DNAV to see whether this RTS should be accepted. If the Rx identifies that there are active nodes in the expected sector, it prepares a DYSA, which denies the established request; otherwise, it prepares a CTS. At the same time, the Tx's other neighbors, who hear the RTS, also check their DNAVs and the NIT. If a neighbor recognizes that the current negotiation will build a link that may collide with certain ongoing data transmission, it prepares a DYSA; otherwise, it keeps silent. Then, the Tx's cooperators with DYSAs enter the cooperation backoff period (CBP) and execute a CSMA-based mechanism. They randomly back off, and the earliest one sends out its veto frame. If the medium is busy after the CBP, which means that there is a DYSA, the Rx cancels its CTS.

If the Tx does not receive CTS, the negotiation ends; otherwise, the Tx prepares the CFA to announce the establishment of a new link. Meanwhile, the Rx's neighbors who hear the CTS also check their DNAVs to see whether they should block the expected link. If a neighbor identifies that this expected link may collide with an ongoing data transmission, it prepares a DYSB. After the CTS, the Rx's cooperators with DYSBs enter the second CBP. If there is no DYSB and CFA is correctly received by the Rx, the Rx sends CFB to confirm link establishment. In some cases that the Tx sends the CFA but receives no CFB, it needs to send CLS to invalidate the previous CFA. Reception of both RTS and CFA (or both CTS and CFB) with no CLS implies successful link establishment. The nodes, which hear the new link establishment, update their DNAVs. With successful negotiation, certain pairs of nodes switch to the data channel and start to transmit after a short interframe space (SIFS). As in the original 802.11, if a data packet is received, the Rx replies with an ACK.

A negotiation, which consists of potential hidden terminals, is stopped by DYSA or DYSB. This solves the multichannel directional hidden terminal problem. Moreover, with reception of DYSA or DYSB, the Tx knows the reason why it cannot start this link and can take further decisions. This solves the deafness problem.

D. Node Cooperation

An example is shown to illustrate how CMDMAC works in Fig. 3. Link 3 was established in data channel 1 during the transmissions of links 1 and 2. After the transmissions of links 1 and 2, B wants to initialize a new transmission to C. Thus, B broadcasts an RTS in the control channel and expects to start the transmission in data channel 2. Upon hearing this RTS, C checks its DNAV and accepts this request with preparing a CTS. At the same time, neighbor G checks its DNAV and NIT and finds that E is active in B's expected sector of the expected data channel. Thus, G backs off and replies a DYSA. Upon receiving the DYSA, B and C know that E is working and may still work for LTIME. Then, B can make its further decision based on the current channel usage situation. As illustrated in this example, neighboring nodes actively cooperate in the process of negotiation to identify the potential hidden terminals and deaf nodes. This helps to solve the hidden terminal and deafness problems asynchronously without additional devices.

VI. Protocol Analysis

Here, we present a theoretical analysis for CMDMAC via three propositions. First, we discuss how minor-lobe interference affects the coexistence condition for directional links. Second, we demonstrate how different antenna beamwidths affect potential spatial sharing gain. Third, we demonstrate that

This article has been accepted for inclusion in a future issue of this journal. Content is final as presented, with the exception of pagination.

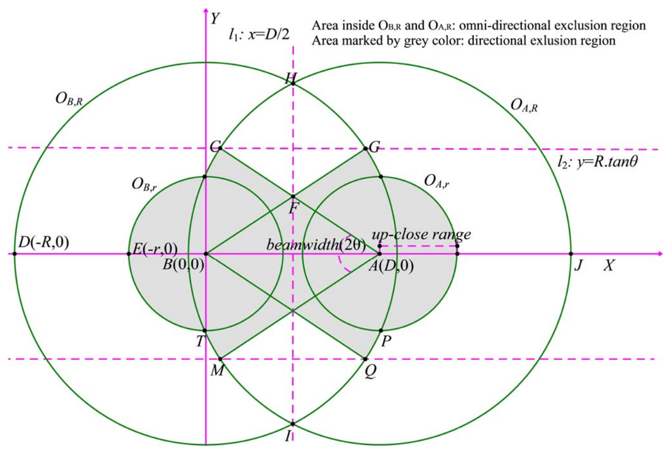

Fig. 7. Exclusion region of omnidirectional and directional transmissions.

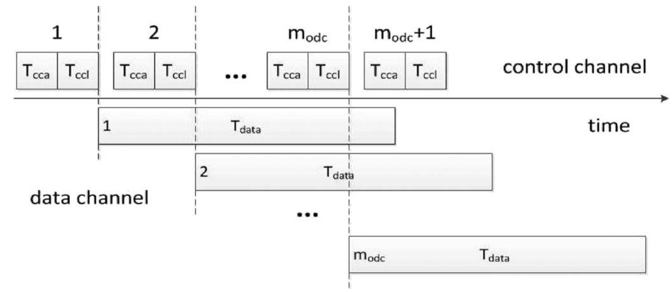

Fig. 8. Illustration of control channel analysis.

a single dedicated control channel can support multichannel directional transmissions.

Proposition 1: Minor-lobe effects of directional antennas change the coexistence condition for directional links.

Proof: We define an exclusion region as a spatial region in a certain channel where no other active terminals exist, except the current active pair of transceivers. The coexistence condition for different links is that they do not lie in other links' exclusion regions. A general case of exclusion region of a link is shown in Fig. 7, where two terminals are located at A and B. The exclusion region of this link in omnidirectional mode is covered by $O_{A,R}$ and $O_{B,R}$. The exclusion region in directional mode is covered by the gray area, which is determined by beamwidth and up-close range. P_t is omnidirectional transmission power; G_m and G_s are gains of the main and minor lobes of directional antenna, respectively; h is the height of antenna; IF_THRESH is the power threshold of interference range. The up-close range r of antenna with minor lobe can be obtained by

$$r = \sqrt[4]{\frac{\frac{P_t}{{G_m}^2} \cdot {G_s}^2 \cdot h^4}{\text{IF\_THRESH}}} \tag{2}$$

given the conditions that $P_T = P_t/{G_m}^2$, $P_R = \text{IF\_THRESH}$, $G_T = G_R = G_s$, and $H_T = H_R = h$ in (1). For any two terminals from different active links in the same channel, if they are in a distance less than or equal to r, they may interfere with each other, resulting in packet conflict. Using ideal antennas with G_s being 0, r is 0, and this terminal's exclusion region is fan shaped. Using nonideal antennas with G_s being nonzero, r is nonzero, and this link's exclusion region is the gray area in Fig. 7. This proposition is discussing the effect of minor lobe. The effect of main lobe will be discussed in Proposition 2.

Proposition 2: Larger beamwidths provide smaller possibility of spatial sharing for directional ad hoc networks.

Proof: This proposition illustrates the benefit of using directional transmission. A main feature of directional transmission is its higher spatial sharing gain (SSG) compared with omnidirectional transmission. We define a metric called possible spatial sharing gain (PSSG), which reflects the possible SSG that directional transmission can provide compared with omnidirectional mode. We use the exclusion region ratio between omnidirectional and directional transmissions to estimate PSSG. As expected, we find that larger beamwidths lead to smaller PSSGs, as shown in Appendix A. With the parameters in our simulation, the PSSG with 30° beamwidth is 2.57, as shown in Appendix B. In the simulations, we find that SSG is about 1.4 in saturation, which is smaller than PSSG. This is due to that PSSG only estimates the possible gain. Real SSG is a case-by-case index and can be affected by many factors, such as network topology and traffic flow.

Proposition 3: One dedicated control channel is capable of coordinating a number of concurrent directional links in a multiple-data-channel scenario.

Proof: This proposition illustrates the capability of using directional and multichannel transmissions together. Using a dedicated channel facilitates terminals to exchange control messages. However, the drawback is that a single control channel may face congestion and become performance bottleneck when there are a large number of terminals in the network. Without losing generality, we suppose a complete communication process that consists of clear channel assessment (CCA), control channel link-establishment handshake, and data channel handshake, as shown in Fig. 8. Without losing generality, we measure the length of CCA and the handshake process in terms of bytes. Thus, particular duration can be obtained dividing length by transmission rate, as follows:

1) T_{cca}: length of a CCA procedure.
2) T_{ccl}: length of a successful control channel link-establishment handshake.
3) T_{data}: length of a successful data channel handshake.

T_{cca} and T_{ccl} are overhead due to the use of CMDMAC. Assume that there are N data channels, the use of control channel leads to bandwidth loss by $1/(N+1)$. The bottleneck problem of control channel is analyzed as follows. We assume that there are a large enough number of data channels in this ad hoc network. We also assume that there are a large number of terminals that are trying to establish links in this network. We define a metric m_{odc} (m_{ddc}) to be the maximum number of omnidirectional (directional) data channels that can be simultaneously used for a given protocol. For m_{odc}, we assume that data transmission is done in omnidirectional mode. Based on Fig. 8, we have

$$m_{\text{odc}} = \left\lceil \frac{T_{\text{data}}}{T_{\text{cca}} + T_{\text{ccl}}} \right\rceil. \tag{3}$$

This article has been accepted for inclusion in a future issue of this journal. Content is final as presented, with the exception of pagination.

As there are a large enough number of data channels, $T_{\rm cca} = T_{\rm cca}^{\rm min}$. As $T_{\rm cca}^{\rm min}$ and $T_{\rm ccl}$ are fixed for CMDMAC, $m_{\rm odc}$ is mainly determined by $T_{\rm data}$, which is dominated by the data payload size. For the directional case, we assume that there are SSG concurrent links in one data channel. We can estimate $m_{\rm ddc}$ as

$$m_{\rm ddc} = \frac{m_{\rm odc}}{\rm SSG}. \tag{4}$$

According to the PHY parameters in our simulation [28], we have $T_{\rm ccl} = 138.5$ bytes, $T_{\rm cca} = 37.5$ bytes, and $T_{\rm data} = 1573.5$ bytes. Thus, we get $m_{\rm odc} = 8.94$. If we take SSG = PSSG, then $m_{\rm ddc}$ is 3.47. However, we find that SSG is around 1.40 and the corresponding $m_{\rm ddc}$ is 6.38 in the simulations. Moreover, if we increase the value of data payload length or use shorter PLCP preamble and headers, CMDMAC can support larger number of data channels. Since both 3.47 and 6.38 are larger than 1, this result demonstrates that one control channel is capable of coordinating multiple links in a multiple data channel network, as described in Proposition 3.

VII. Performance Evaluation

Here, we evaluate the performance of CMDMAC using NS-2. For comparison, we define a noncooperative version of CMDMAC, which is called noncooperation directional MAC (NCDMAC). The only difference between CMDMAC and NCDMAC is whether the neighboring nodes cooperate in solving the hidden terminal and deafness problems. Specifically in NCDMAC, the neighboring nodes do not send DYSA/DYSB to cooperate. We also compare with omnidirectional 802.11 protocol provided by NS-2.

A. Simulation Configuration

The simulation parameters are shown in Table I. The transmission and interference ranges are determined by the value of G_m/G_s for the two-ray propagation model. By adapting Tx powers for control and data channel, the transmission ranges in both control and data channel are made 250 m. K nodes are randomly located, and K nondisjoint User Datagram Protocol (UDP) flows with constant rate are generated as data sources, where each node is the source and destination of one flow. The capture effect is implemented based on the comparison of reception power in NS-2. In the existing benchmarks [3], [7], [22], 10–20 random network scenarios are considered. In this paper, 20 random scenarios are generated, and each performance measurement reported in the following is averaged over the results from the 20 scenarios. Simulation duration is set as 200 s, since it is enough for initial network setting such as neighbor discovering and entering into data transmission period.

Two performance metrics are examined to compare CMDMAC and NCDMAC: end-to-end (aggregate) throughput, which is defined as the total data delivered from source to destination divided by the simulation duration, and packet error rate (PER), which is defined as the ratio of number of packets not correctly received to number of packets sent in MAC layer. We use average aggregate throughput as it is a popular metric. Generally speaking, the average delay is data transmitted divided by overall transmission rate. Thus, the average delay is reflected by the throughput. The detail information about latency issue will be studied in future work. We use PER as it is a one-hop metric and can reflect how much our cooperation reduces the data packet collisions. We also talk about saturation break point as the point before which all the data demands can be satisfied. Packets may accumulate and queue occupancy may grow at some nodes after this point.

TABLE I
Simulation Parameters

Simulator	NS-2
Tx power (CC/DC)	24.5 dBm/ 4.5 dBm
Rx threshold	-64.375 dBm
Capture threshold	10 dB
Transmission rate	1 Mbps
Cooperation backoff period	40 μs
G_m/G_s	10 dB
Propagation model	two-ray model
Topology dimensions	500 m * 500 m
Simulation time	120 s

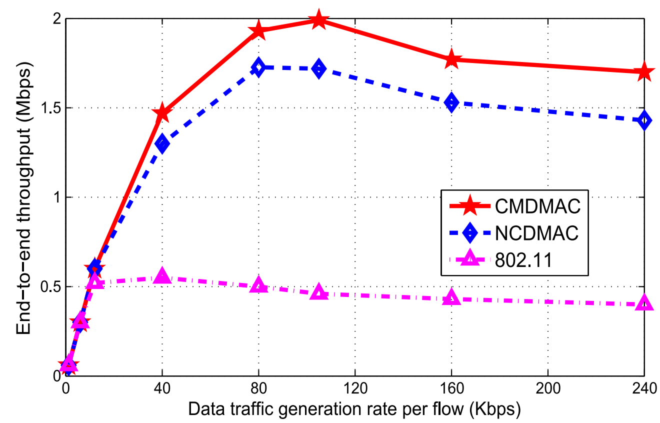

Fig. 9. Impact of traffic load.

B. Single-Data-Channel Scenario

Here, we show simulation results of scenarios with a single data channel. The impact of traffic load, packet sizes, and beamwidths is examined.

In Fig. 9, the impact of traffic loads is shown with 50 nodes, 30 beamwidth and 1500-byte packet size. It is clear that CMDMAC outperforms NCDMAC.

In Fig. 10, the impact of node densities is shown with 100 Kbps traffic per flow, 30 beamwidth and 1500-byte payload. We see that difference between CMDMAC and NCDMAC is smaller when node density is low as compared to that when node density is high. It is expected that there will be fewer packet conflicts when node density is low, thus CMDMAC may not bring much benefit.

In Fig. 11, the impact of different beamwidths is shown with 50 nodes, 240 Kbps date rate (50 flows) and 15 to 90 beamwidths. We see that the throughput with wider beamwidths are smaller than that with narrower beamwidths due to that narrower beamwidths provide more co-existence links which support larger throughput as explained in Proposition 2.

This article has been accepted for inclusion in a future issue of this journal. Content is final as presented, with the exception of pagination.

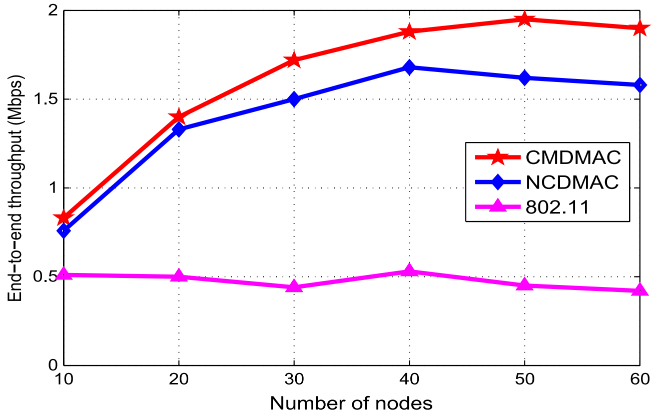

Fig. 10. Impact of node density.

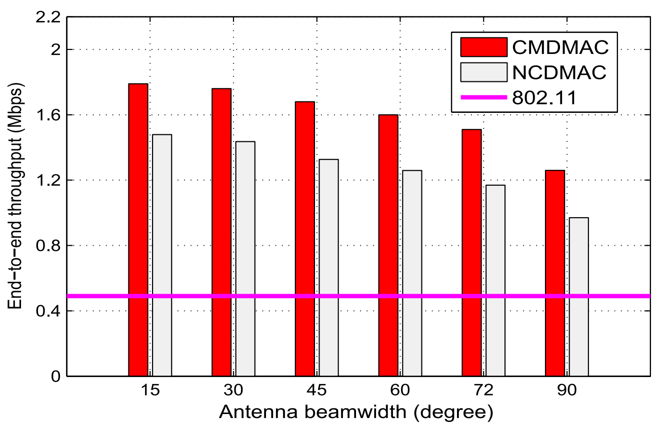

Fig. 11. Impact of beamwidth.

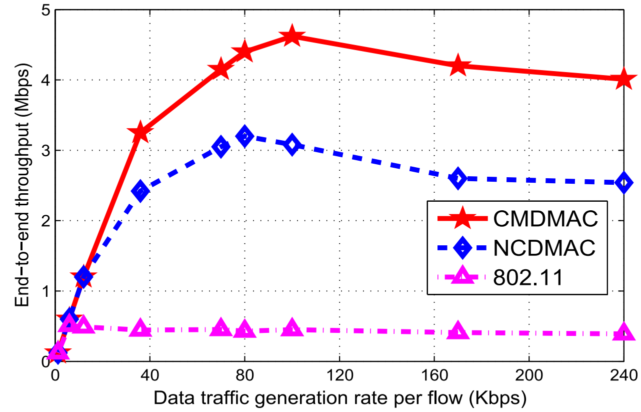

(a)

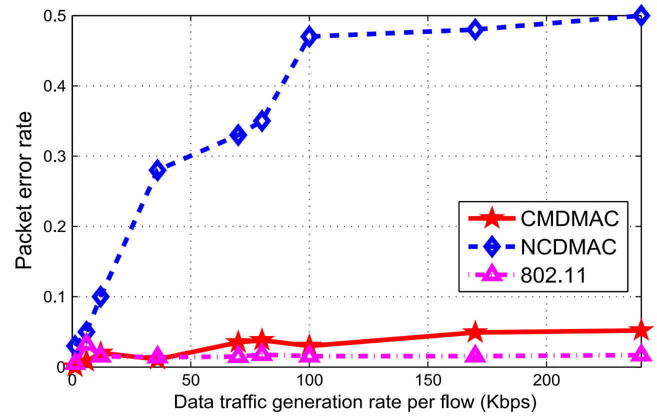

(b)

Fig. 12. Impact of traffic load for multiple-data-channel scenario. (a) Throughput with different traffic loads. (b) PER with different traffic loads.

C. *Multiple-Data-Channel Scenario*

Here, we show the simulation results for the multiple-data-channel scenario. We study the impact of traffic load, data packet sizes, and channel numbers.

In Fig. 12, the impact of traffic loads is shown with 100 nodes, 4 data channels, 30 and 1500-byte packet payload. In Fig. 12(a), the basic trends of throughput performance are very similar as those with a single data channel. However, the difference between CMDMAC and NCDMAC is much larger than that in the single-data-channel scenario. The reason is as follows. In the single-data-channel case, a Tx with CMDMAC reaps benefit only from DYSA/DYSB by canceling its wrong negotiation. Then, the Tx does nothing but waits for the ongoing links to end. However, in the multi-data-channel case, this Tx reaps benefit in two fold: i) cancel current negotiation; and ii) back off and then initialize a new negotiation for another potentially free channel immediately. In Fig. 12(b), we see that CMDMAC outperforms NCDMAC for all cases and NCDMAC's PER keeps increasing as traffic load becomes higher.

In Fig. 13, the impact of different data payloads is shown with 100 nodes, 240 Kbps traffic load, 4 data channels and 30 beamwidth. In Fig. 13(a), the end-to-end throughput keeps increasing with larger packet sizes. Both CMDMACand NCDMAC benefit from larger data packet sizes because the larger packet size offsets handshake overheads more effectively. With larger size packets, the number of packets reduces. Meanwhile, the collision of one packet becomes more harmful to throughput. In Fig. 13(b), PERs are stable around 5% for both CMDMAC and 802.11. For NCDMAC, it first increases and then slowly decreases. This phenomenon is due to two contradicting factors: longer data packets are more susceptible to channel conflicts; longer data packets keep nodes on data channels longer hence fewer nodes will be able to start new communication which reduces the possibility of channel conflicts.

In Fig. 14, the impact of different data channel numbers is shown with 100 nodes, 240 Kbps traffic load per flow, 30 beamwidth and packet payload size is 1500 bytes. In Fig. 14(a), we see that aggregate throughput increases with the number of data channels. This is as predicted in to Proposition 3. Since aggregate throughput is an end-to-end issue and can be affected by topology, routing protocol and many other factors in addition to MAC, we are not surprised that the increase is not linear with the number of data channels. In Fig. 14(b), we show PER for CMDMAC, NCDMAC and 802.11. While 802.11 provides nearly 2% PER, that of CMDMAC is around 5%. For NCDMAC, PER increases with more data channels at first. As the number of data channel keeps increasing to 5, the PER starts to reduce slightly. To understand this, we assume there are an infinite number of data channels. Then, the collision possibility should be zero as each link can get a free channel. This special case gives the hint for the slight decrease with 5 data channels.

This article has been accepted for inclusion in a future issue of this journal. Content is final as presented, with the exception of pagination.

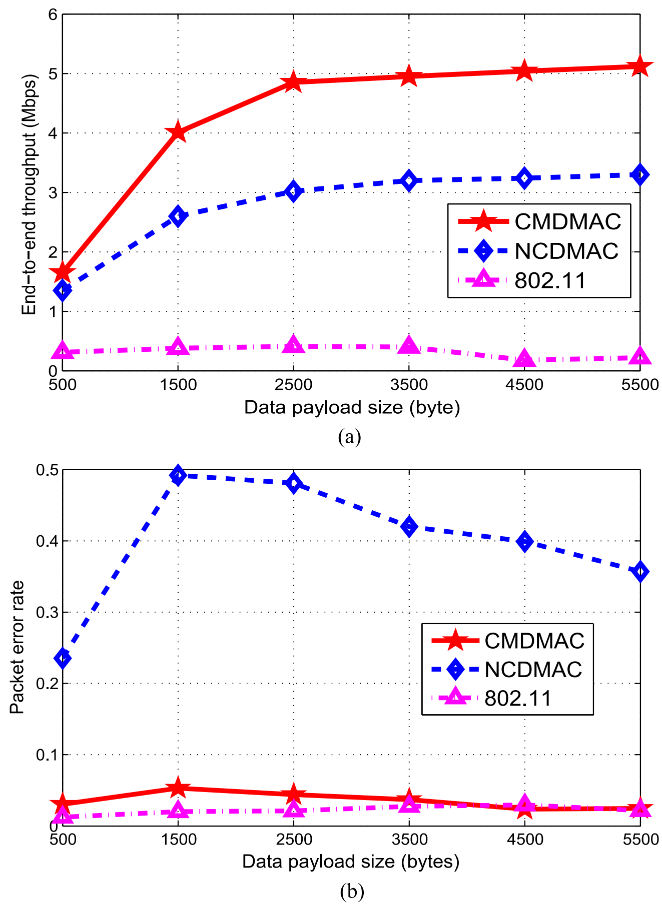

Fig. 13. Impact of data payload size for multiple-data-channel scenario. (a) Throughput with different data payload sizes. (b) PER with different data payload sizes.

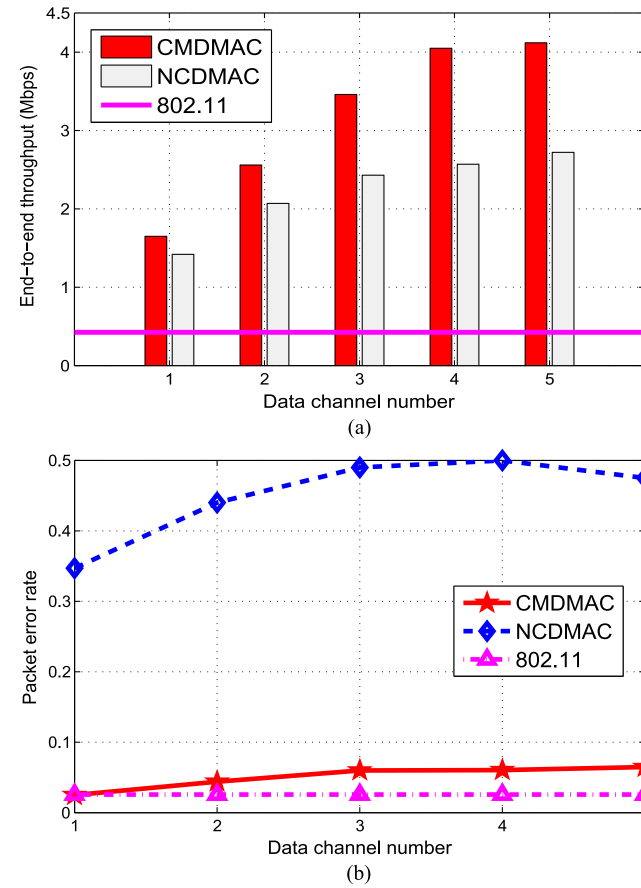

Fig. 14. Impact of number of data channels for multiple-data-channel scenario. (a) Throughput with different data channel numbers. (b) PER with different data channel numbers.

D. Mobile Scenario

In Fig. 15, the impact of mobility is studied for both single- and multiple-channel scenarios. The traffic load per flow is set to 240 kb/s. The numbers of nodes are 50 and 100 for one and four data channels, respectively. The beamwidth is set as 30°, and the traffic load is 240 kb/s. The topology dimension is 500 m × 500 m. The packet payload size is 1500 bytes. The NIT updating mechanism in Section V-B is used. Compared with static scenario [see Fig. 14(a)], the performance degradation is about 11% for the single-data-channel case and 15% for the multi-data-channel case, at a speed of 4 m/s. This is due to that the cooperators do not have the correct location information. Thus, they may fail to recognize the potential hidden terminals or they may deny the negotiation, which should be permitted. Both these two actions may harm the performance.

E. Comparisons With DMAC, CDMAC, MMAC, and CAMMAC

We compare CMDMAC with other benchmark directional MACs and multichannel MACs. As we cannot compare with all the existing protocols, we perform a comparison with the more popular benchmark protocols, which provide clear algorithm description and simulation settings. Therefore, it is convenient for future researchers to compare our work with other unmentioned protocols who also compare to those benchmark studies. All of the comparisons use a single half-duplex transceiver, whereas CDMAC [12] and MMAC [16] require clock synchronization. For the purpose of comparison, all results are with the same parameters settings as reported in the relevant papers.

1) Comparison With DMAC [2]: DMAC is proposed for asynchronous directional networks. The number of nodes is fixed while the network size is adjusted according to the nodes densities in this comparison. In Fig. 16, M represents the sector number. 25 nodes are deployed randomly and 25 flows are initiated. It is assume that there is only 1 data channel and channel capacity is 2 Mbps. Packet size is 1000 bytes and Traffic load per flow is set as 25 packet/second. CMDMAC outperforms DMAC in terms of throughput with both 45 and 90 beamwidths for all the nodes densities. The shortfall of DMAC is mainly in the carrier sensing scheme. Although directional virtual carrier sensing is proposed in DMAC design, this function is not comprehensive and DMAC mainly depends on pure carrier sensing to determine whether the channel is available. With this kind of carrier sensing approach, DMAC cannot solve the deafness and hidden terminal problems properly. One channel is needed to implement DMAC, while at least two channels are needed to implement CMDMAC. There are multiple channels available in the unlicensed band, for example 802.11a has twelve channels. Therefore, it is no problem if one of them is dedicated as the

This article has been accepted for inclusion in a future issue of this journal. Content is final as presented, with the exception of pagination.

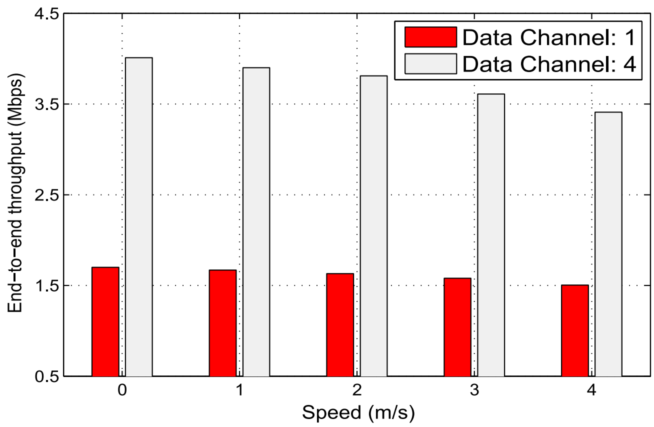

Fig. 15. Impact of mobility.

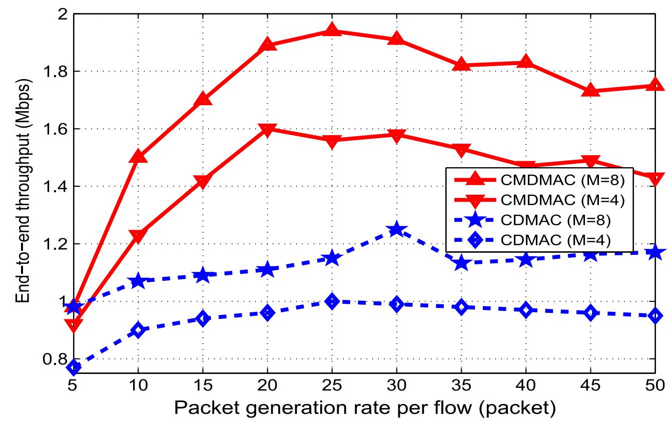

Fig. 17. Comparison with CDMAC.

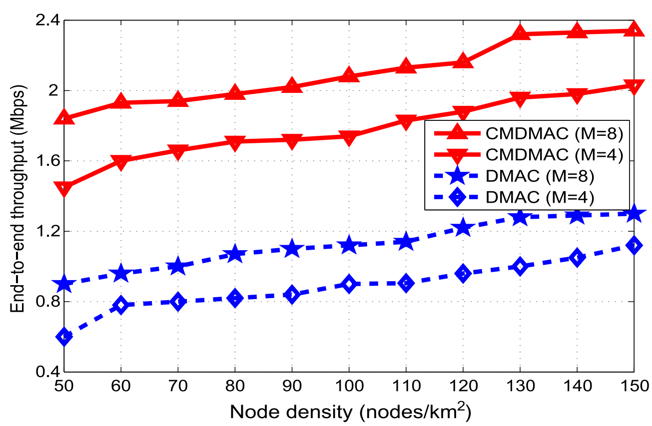

Fig. 16. Comparison with DMAC.

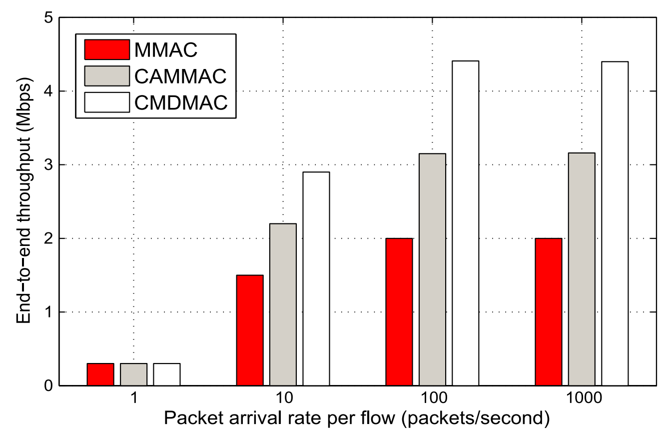

Fig. 18. Comparison with MMAC and CAMMAC.

control channel. Moreover, CMDMAC can work in a multichannel scenario and benefit from the multiple data channels, while DMAC does not do that.

2) Comparison With CDMAC [12]: CDMAC is proposed for synchronous directional networks by using contention window. The packet generation rate is varied from 5 to 50. In Fig. 17, M represents the sector number. 25 nodes are deployed randomly in a 645 meters by 645 meters area. There is 1 data channel with capacity as 2 Mbps. Packet size is set as 1000 bytes. Ratio of Gm towards Gs is set as 30 dB. And the flow number is 25. For both CMDMAC and CDMAC, it is not surprising that narrower beamwidths provide better performance by providing higher spatial sharing possibilities. Also, it is shown that CDMAC quickly saturates with higher packet generation rate, while CMDMAC can provide about 56% and 60% larger throughput performance than CDMAC (M=8) and CDMAC (M=4) respectively. The advantage of CMDMAC also comes with solving the hidden terminal problem. In CDMAC, the network is divided into a master-slave structure. While the deafness and hidden terminal problems are solved within a local group hosted by a master, there will be packet collisions at the borders of different groups. Moreover, to deliver a packet from one group to another, a node has to wait for a long time to join another group. Further, since CDMAC uses clock synchronization and divides the time into master node selection window, slaves iterative contention window and data transmission window, it is hard to decide the optimum values of the window sizes.

3) Comparison With MMAC [16] and CAMMAC [22]: We compare our CMDMAC to two multichannel MACs, namely, MMAC and CAMMAC. In this comparison, CMDMAC and CAMMAC use three data channels to maintain the fairness toward MMAC. CMDMAC uses a 30° antenna beam. MMAC needs clock synchronization. In Fig. 18, 100 nodes are randomly deployed in a 500 m × 500 m area. Forty data flows are initiated in the network. G_m/G_s for each antenna is 10 dB, and sector width is 30°. There are four channels with 2-Mb/s capacity. Packet size is 1024 bytes. We see that these three MACs have the same throughput for light-load networking scenarios. For the saturated case, CMDMAC achieves about 2.23 times the throughput of MMAC. While CAMMAC can be understood as an omnidirectional version of CMDMAC, CMDMAC with 30° achieves about 1.40 times the throughput of CAMMAC. This is due to the SSG provided by directional transmission.

VIII. Conclusion

Observing that multiple radios or network-wide synchronization may not be available in directional ad hoc networks, we have proposed CMDMAC, which employs single radio to solve deafness and hidden terminal problems asynchronously. In CMDMAC, idle terminals in the control channel actively participate in the negotiation procedures of their neighbors and help them identify available data channels. Theoretical analysis is provided, and NS-2 simulations are used to validate the protocol's performance. Comparison with popular benchmarks shows that CMDMAC reduces PER effectively and provides better throughput performance.

Appendix A
Proof of Proposition 2

$O_{A,R}$ and $O_{A,r}$ are used to represent the concentric circles with their centers at A. $O_{B,R}$ and $O_{B,r}$ are used to represent the concentric circles with their centers at B. For simplicity, we set R equal to 1. With α being $\operatorname{arccot}(D/2)$, the area $S_{A,B}$ covered by $O_{A,R}$ and $O_{B,R}$ is

$$S_{A,B}(D) = 2\pi - 2\alpha + D \cdot \sin(\alpha). \tag{5}$$

The gray area, which is the exclusion region of this link, is symmetrical about both the X- and Y-axes. For the gray part in the range of $x \in (-\infty, D/2]$ and $y \in [0, +\infty)$, it is $1/4$ of the whole gray area and is named S_{CS}. S_{CS} is determined by r, D, and θ. In Fig. 7, it is clear that the function of line AC is

$$y = f_1(x, D, \theta) : y = (D - x) \cdot \tan(\theta). \tag{6}$$

The function of $O_{A,R}$ is

$$y = f_2(x, D) : y^2 + (x + D)^2 = R^2. \tag{7}$$

The function of $O_{B,r}$ is

$$y = f_3(x) : y^2 + x^2 = r^2. \tag{8}$$

We set

$$y = f_4(x, D, \theta) : y = \max\left(f_1(x, D, \theta), f_2(x, D), f_3(x)\right). \tag{9}$$

For D (or x) outside certain function's definition domain, the value of this function is deemed as 0 in (9). For the reason that S_{CS} is related to D, we have

$$S_{CS}(D, \theta) = \int_{\min(-r, D-R)}^{\frac{D}{2}} f_4(x, D, \theta) dx. \tag{10}$$

For certain $x \in (\infty, D/2, D \in [0, R]$, and $\theta_1 \geq \theta_2$, we have

$$f_1(x, D, \theta_1) \geq f_1(x, D, \theta_2). \tag{11}$$

Therefore, we have

$$f_4(x, D, \theta_1) \geq f_4(x, D, \theta_2) \tag{12}$$

$$S_{CS}(D, \theta_1) \geq S_{CS}(D, \theta_2). \tag{13}$$

For the PSSG, we have

$$\frac{S_{A,B}(D)}{S_{CS}(D, \theta_1)} \leq \frac{S_{A,B}(D)}{S_{CS}(D, \theta_2)}. \tag{14}$$

For the averaged PSSG, we have

$$f_{\text{PSSG}}(\theta) = \frac{1}{R} \cdot \int_0^R \frac{S_{A,B}(D)}{4 \cdot S_{CS}(D, \theta)} dD. \tag{15}$$

Based on (14) and (15), we have

$$f_{\text{PSSG}}(\theta_1) \leq f_{\text{PSSG}}(\theta_2). \tag{16}$$

Equation (16) means that the PSSG becomes smaller with larger θ, which illustrate why wider antenna beams bring smaller SSGs.

Appendix B
PSSG

D is the distance between $O_{B,R}$ and $O_{A,R}$. For simplicity, we assume R to be 1. With our system model and based on (2), we get r as 0.5619. The beamwidth is now 30°. The function of the $O_{B,r}$, l_{AC}, and $O_{A,R}$ above the x-axis is as follows:

$$\begin{cases} g_1(x) = \sqrt{r^2 - x^2} \\ g_2(x) = \tan\left(\frac{\pi}{12}\right) \cdot (D - x) \\ g_3(x) = \sqrt{1 - (x - D)^2}. \end{cases} \tag{17}$$

The exclusion region of directional transmission with $D \in [0, 0.4381)$ is similar to Fig. 7, and its area is as follows:

$$f_1(D) = 4 \cdot \left[\int_{x_1}^{x_0} g_1(x) dx + \int_{x_2}^{x_1} g_2(x) dx + \int_{x_3}^{x_2} g_3(x) dx \right] \tag{18}$$

where

$$\begin{cases} x_0 = \frac{D}{2} \\ x_1 = \frac{2D \cdot \tan^2\left(\frac{\pi}{12}\right) - \sqrt{4D^2 \cdot \tan^4\left(\frac{\pi}{12} + 1\right) \cdot \left(D^2 \cdot \tan^2\left(\frac{\pi}{12}\right) - r^2\right)}}{2 \cdot \left(\tan^2\left(\frac{\pi}{12}\right) + 1\right)} \\ x_2 = D - \cos\left(\frac{\pi}{12}\right) \\ x_3 = D - 1. \end{cases} \tag{19}$$

For $D \in [0.4381, 0.4671)$, the exclusion region is

$$f_2(D) = 4 \cdot \left[\int_{x_1'}^{x_0'} g_1(x) dx + \int_{x_2'}^{x_1'} g_2(x) dx + \int_{x_3'}^{x_2'} g_3(x) dx + \int_{x_4'}^{x_3'} g_1(x) dx \right] \tag{20}$$

where

$$\begin{cases} x_0' = \frac{D}{2} \\ x_1' = \frac{2D \cdot \tan^2\left(\frac{\pi}{12}\right) - \sqrt{4D^2 \cdot \tan^4\left(\frac{\pi}{12} + 1\right) \cdot \left(D^2 \cdot \tan^2\left(\frac{\pi}{12}\right) - r^2\right)}}{2 \cdot \left(\tan^2\left(\frac{\pi}{12}\right) + 1\right)} \\ x_2' = D - \cos\left(\frac{\pi}{12}\right) \\ x_3' = \frac{D^2 + r^2 - 1}{2D} \\ x_4' = -r. \end{cases} \tag{21}$$

For $D \in [0.4671, 1]$, the exclusion region is

$$f_3(D) = 2\pi r^2 - 2r^2 \cdot a\cos\left(\frac{D}{2r}\right) + r \cdot D \cdot \sin\left(a\cos\left(\frac{D}{2r}\right)\right). \tag{22}$$

The exclusion region of the omnidirectional transmission link is

$$f_4(D) = 2\pi - 2 \cdot a\cos\left(\frac{D}{2}\right) + D \cdot \sin\left(a\cos\left(\frac{D}{2}\right)\right). \tag{23}$$

Based on (15), the PSSG with 30° beam is

$$\text{PSSG} = \int_0^{0.4381} \frac{f_4(D)}{f_1(D)} dD + \int_{0.4381}^{0.4671} \frac{f_4(D)}{f_2(D)} dD + \int_{0.4671}^{1} \frac{f_4(D)}{f_3(D)} dD. \tag{24}$$

Using MATLAB, we get the numerical value of 2.57.

ACKNOWLEDGMENT

This research was carried out at the National University of Singapore-Zhejiang University Sensor-Enhanced Social Media Centre.

REFERENCES

[1] Y. Wang, M. Motani, H. K. Garg, Q. Chen, and T. Luo, “Multi-channel directional medium access control for ad hoc networks: A cooperative approach,” in *Proc. IEEE ICC*, Sydney, Australia, Jun. 2014, pp. 53–58.

[2] M. Takai, J. Martin, A. Ren, and R. Bagrodia, “Directional virtual carrier sensing for directional antennas in mobile ad hoc networks,” in *Proc. ACM Int. Symp. MobiHoc*, Lausanne, Switzerland, Jun. 2002, pp. 183–193.

[3] R. Choudhury, X. Yang, R. Ramannathan, and N. Vaidya, “On designing MAC protocols for wireless networks using directional antennas,” *IEEE Trans. Mobile Comput.*, vol. 5, no. 5, pp. 477–491, May 2006.

[4] Y. Takatsuka, M. Takata, M. Bandai, and T. Watanabe, “A MAC protocol for directional hidden terminal and minor lobe problems,” in *Proc. Wireless Telecommun. Symp.*, Pomona, CA, Canada, Apr. 2008, pp. 210–219.

[5] J. Chang, W. Liao, and J. Lai, “On reservation-based MAC protocol for IEEE 802.11 wireless ad hoc networks with directional antenna,” *IEEE Trans. Veh. Technol.*, vol. 60, no. 6, pp. 2669–2679, Jul. 2011.

[6] A. Arora, M. Krunz, and A. Muqattash, “Directional medium access protocol with power control for wireless ad hoc networks,” in *Proc. IEEE GLOBECOM*, Dec. 2004, pp. 2797–2801.

[7] T. Korakis, G. Jakllari, and L. Tassiulas, “CDR-MAC: A protocol for full exploitation of directional antennas in ad-hoc wireless networks,” *IEEE Trans. Mobile Comput.*, vol. 7, no. 2, pp. 145–155, Feb. 2008.

[8] W. Na, L. Park, and S. Cho, “Deafness-aware MAC protocol for directional antennas,” in *Proc. IEEE ICCE*, Las Vegas, NV, USA, Jan. 2013, pp. 625–626.

[9] S. Motegi, H. Sekiya, J. Ma, K. Sanada, and S. Sakara, “Directional MAC protocol with DATA-frame fragmentation and short busy advertisement signal for mitigating the directional hidden node problem,” in *Proc. IEEE Int. Symp. PIMRC*, Sydney, NSW, Australia, Sep. 2012, pp. 393–398.

[10] A. Abdullah, L. Cai, and F. Gebali, “DSDMAC: Dual sensing directional MAC protocol for ad hoc networks with directional antennas,” *IEEE Trans. Veh. Technol.*, vol. 61, no. 3, pp. 1266–1275, Mar. 2012.

[11] Q. Jian, X. Lin, X. Shen, and J. Mark, “Enabling multi-hop concurrent transmissions in 60 GHz wireless personal area networks,” *IEEE Trans. Wireless Commun.*, vol. 10, no. 11, pp. 3824–3833, Nov. 2011.

[12] J. Wang, H. Zhai, P. Li, Y. Fang, and D. Wu, “Directional medium access control for ad hoc networks,” *Springer Wireless Netw.*, vol. 15, no. 8, pp. 1059–1073, Nov. 2009.

[13] A. Adya, P. Bahl, J. Padhye, and A. Wolman, “A multi-radio unification protocol for IEEE 802. 11 wireless networks,” in *Proc. IEEE Int. Conf. BroadNets*, San Jose, CA, USA, Oct. 2004, pp. 344–354.

[14] R. Maheshwari, H. Gupta, and S. Das, “Multi-channel MAC protocols for wireless networks,” in *Proc. IEEE SECON*, Reston, VA, USA, Sep. 2006, pp. 393–401.

[15] J. Chen, S. Sheu, and C. Yang, “A new multichannel access protocol for IEEE 802.11 ad hoc wireless LANs,” in *Proc. IEEE PIMRC*, Beijing, China, Sep. 2003, pp. 2291–2296.

[16] J. So and N. Vaidya, “Multi-channel MAC for ad hoc networks: Handling multi-channel hidden terminals using a single transceiver,” in *Proc. ACM MobiHoc*, Tokyo, Japan, May 2004, pp. 222–233.

[17] A. Tzamaloukas and J. Garcia-Luna-Aceves, “Channel-hopping multiple access,” in *Proc. IEEE ICC*, New Orleans, LA, USA, Jun. 2000, pp. 415–419.

[18] H. So, G. Nguyen, and J. Walrand, “Practical synchronization techniques for multi-channel MAC,” in *Proc. ACM MobiCom*, Sep. 2006, pp. 134–145.

[19] A. Acharya, A. Misra, and S. Bansal, “Design and analysis of a cooperative medium access scheme for wireless mesh networks,” in *Proc. IEEE BroadNets*, Oct. 2004, pp. 621–631.

[20] K. Tan, Z. Wan, H. Zhu, and J. Andrian, “CODE: Cooperative medium access for multirate wireless ad hoc network,” in *Proc. IEEE SECON*, San Diego, CA, USA, Jun. 2007, pp. 1–10.

[21] T. Guo and R. Carrasco, “CRBAR: Cooperative relay-based auto rate MAC for multirate wireless networks,” *IEEE Trans. Wireless Commun.*, vol. 8, no. 12, pp. 5938–5947, Dec. 2009.

[22] T. Luo, M. Motani, and V. Srinivasan, “Cooperative asynchronous multichannel MAC: Design, analysis, and implementation,” *IEEE Trans. Mobile Comput.*, vol. 8, no. 3, pp. 338–352, Mar. 2009.

[23] X. Zhang and H. Su, “CREAM-MAC: Cognitive radio-enabled multichannel MAC protocol over dynamic spectrum access networks,” *IEEE J. Sel. Topics Signal Process.*, vol. 5, no. 1, pp. 110–123, Feb. 2011.

[24] W. Jeon, J. Han, and D. Jeong, “A novel MAC scheme for multichannel cognitive radio ad hoc networks,” *IEEE Trans. Mobile Comput.*, vol. 11, no. 6, pp. 922–934, Apr. 2012.

[25] M. Timmers, S. Pollin, A. Dejonghe, L. Perre, and F. Catthoor, “A distributed multichannel MAC protocol for multihop cognitive radio networks,” *IEEE Trans. Veh. Technol.*, vol. 59, no. 1, pp. 446–459, Jan. 2010.

[26] L. Tan and L. L, “Distributed MAC protocol for cognitive radio networks: Design, analysis, and optimization,” *IEEE Trans. Veh. Technol.*, vol. 60, no. 8, pp. 3990–4003, Oct. 2011.

[27] R. Ramanathan, “On the performance of beamforming antennas in ad hoc networks,” in *Proc. ACM MobiHoc*, Long Beach, CA, USA, Oct. 2001, pp. 95–105.

[28] *Wireless LAN Medium Access Control (MAC) and Physical Layer (PHY) Specifications*, IEEE Std. 802.11a-1999, Dec. 1999.

Yu Wang received the Ph.D. degree in electrical and computer engineering from the National University of Singapore, Singapore.

He is currently with the Department of Electrical and Computer Engineering, National University of Singapore. His research interests are in wireless protocols for computer networks.

Mehul Motani (S’92–M’01–SM’15) received the B.E. degree from The Cooper Union, New York, NY, USA, the M.S. degree from Syracuse University, Syracuse, NY, and the Ph.D. degree from Cornell University, Ithaca, NY, all in electrical and computer engineering.

He is currently an Associate Professor with the Department of Electrical and Computer Engineering, National University of Singapore, Singapore. He has broad research interests and likes research problems which sit at the boundary of information theory, computing, networking, and communications.

Hari Krishna Garg received the Ph.D. degree from Concordia University, Montréal, Canada, and the MBA degree from Syracuse University, Syracuse, NY, USA.

He is currently with the Department of Electrical and Computer Engineering, National University of Singapore, Singapore. His research interests are in the areas of cellular/mobile/wireless communications, digital signal/image processing, coding theory, and digital watermarking. He has coauthored a number of books on topics in digital signal processing.

Qian Chen (M’09) received the Ph.D. degree in electrical and computer engineering from the National University of Singapore, Singapore.

He is currently a Scientist with the Institute for Infocomm Research, Singapore.

Tie Luo (M’09) received the Ph.D. degree in electrical and computer engineering from the National University of Singapore, Singapore.

He is currently a Scientist with the Institute for Infocomm Research, Singapore.